AFRL-PR-WP-TP-2006-239

VALIDATION OF HEAT- FLUX PREDICTIONS ON THE OUTER AIR SEAL OF A TRANSONIC TURBINE BLADE (Preprint)

John P. Clark, Marc D. Polanka, and Matthew Meininger (AFRL/PRTT)
Thomas J. Praisner (United Technologies Corp., Pratt & Whitney)

June 2006

Approved for public release; distribution is unlimited.

STINFO COPY

PROPULSION DIRECTORATE
AIR FORCE RESEARCH LABORATORY
AIR FORCE MATERIEL COMMAND
WRIGHT-PATTERSON AIR FORCE BASE, OH 45433-7251

REPORT DOCUMENTATION PAGE

1. REPORT DATE *(DD-MM-YY)*	2. REPORT TYPE	3. DATES COVERED *(From - To)*
June 2006	Journal Article Preprint	06/15/2005 – 01/15/2006

4. TITLE AND SUBTITLE

VALIDATION OF HEAT- FLUX PREDICTIONS ON THE OUTER AIR SEAL OF A TRANSONIC TURBINE BLADE (Preprint)

5a. CONTRACT NUMBER
In-House

5b. GRANT NUMBER

5c. PROGRAM ELEMENT NUMBER
62203F

6. AUTHOR(S)

John P. Clark, Marc D. Polanka, and Matthew Meininger (AFRL/PRTT)
Thomas J. Praisner (United Technologies Corp., Pratt & Whitney)

5d. PROJECT NUMBER
3066

5e. TASK NUMBER
06

5f. WORK UNIT NUMBER
WS

7. PERFORMING ORGANIZATION NAME(S) AND ADDRESS(ES)

Turbine Branch (AFRL/PRTT)
Turbine Engine Division
Propulsion Directorate
Air Force Research Laboratory, Air Force Materiel Command
Wright-Patterson AFB, OH 45433-7251

United Technologies Corp.
Pratt & Whitney
East Hartford, CT 06108

8. PERFORMING ORGANIZATION REPORT NUMBER

AFRL-PR-WP-TP-2006-239

9. SPONSORING/MONITORING AGENCY NAME(S) AND ADDRESS(ES)

Propulsion Directorate
Air Force Research Laboratory
Air Force Materiel Command
Wright-Patterson AFB, OH 45433-7251

10. SPONSORING/MONITORING AGENCY ACRONYM(S)
AFRL-PR-WP

11. SPONSORING/MONITORING AGENCY REPORT NUMBER(S)
AFRL-PR-WP-TP-2006-239

12. DISTRIBUTION/AVAILABILITY STATEMENT
Approved for public release; distribution is unlimited.

13. SUPPLEMENTARY NOTES

14. ABSTRACT

It is desirable to predict accurately the heat load on turbine hot section components within the design cycle of the engine. So, a set of predictions of the heat flux on the Blade Outer Air Seal (BOAS) of a transonic turbine is here validated with time-resolved measurements obtained in a single-stage high pressure turbine rig. Surface pressure measurements were also obtained along the blade outer air seal, and these are also compared with 3-D, Reynolds-averaged Navier-Stokes predictions. A region of very high heat flux was predicted as the pressure side of the blade passed a fixed location on the blade outer air seal, but this was not measured in the experiment. The region of high heat flux was associated both with very high harmonics of the blade-passing event and a discrepancy between predicted and measured time-mean heat-flux levels. Further analysis of the predicted heat flux in light of the experimental technique employed in the test revealed that the elevated heat flux associated with passage of the pressure side might be physical. Improvements in the experimental technique are suggested for future efforts.

15. SUBJECT TERMS
turbine blades, thermal conductivity, fraction of blade axial chord, law-of-the-wall variable, adiabatic wall

16. SECURITY CLASSIFICATION OF:			17. LIMITATION OF ABSTRACT:	18. NUMBER OF PAGES	19a. NAME OF RESPONSIBLE PERSON (Monitor)
a. REPORT Unclassified	**b. ABSTRACT** Unclassified	**c. THIS PAGE** Unclassified	SAR	24	John P. Clark
					19b. TELEPHONE NUMBER *(Include Area Code)* (937) 255-7152

Validation of Heat-Flux Predictions on the
Outer Air Seal of a Transonic Turbine Blade (Preprint)

John P. Clark, Marc D. Polanka, and Matthew Meininger
Air Force Research Laboratory
Turbine Branch
WPAFB, Ohio 45433

Thomas J. Praisner
United Technologies, Pratt & Whitney
East Hartford, CT 06108

It is desirable to predict accurately the heat load on turbine hot section components within the design cycle of the engine. So, a set of predictions of the heat flux on the Blade Outer Air Seal (BOAS) of a transonic turbine is here validated with time-resolved measurements obtained in a single-stage high pressure turbine rig. Surface pressure measurements were also obtained along the blade outer air seal, and these are also compared with 3-D, Reynolds-averaged Navier-Stokes predictions. A region of very high heat flux was predicted as the pressure side of the blade passed a fixed location on the blade outer air seal, but this was not measured in the experiment. The region of high heat flux was associated both with very high harmonics of the blade-passing event and a discrepancy between predicted and measured time-mean heat-flux levels. Further analysis of the predicted heat flux in light of the experimental technique employed in the test revealed that the elevated heat flux associated with passage of the pressure side might be physical. Improvements in the experimental technique are suggested for future efforts.

INTRODUCTION

For future gas turbine engines, it is desirable both to increase performance and to reduce operating costs. While turbine performance increases are achievable through increases in turbine inlet temperature, this often results in decreased turbine durability. Since designers typically rely on an experience-based approach, there is a durability margin that is built into the design of turbine components. Consequently, component life estimates can either be over-predicted or under-predicted. If part life is over-predicted, then turbine components are using more than the optimum amount of cooling, and the performance of the overall system is reduced perforce. However, if part life is under-predicted, then the system requires more

frequent inspection coupled with possible repairs and/or part replacements. This inevitably results in increased life-cycle costs as well as reduced readiness of the armed forces. The prediction of turbine BOAS region cooling requirements contains an especially significant amount of empiricism. So, a better fundamental understanding of the complex flow and thermal environment in this region is critical to improving the predictive capability that will allow minimization of cooling at desired durability and performance levels.

As detailed in the review article of Dunn [1], several researchers have predicted the flow in the near-blade-tip region, over the tip, and on the Blade Outer Air Seal (BOAS), but very few studies that focus on time-resolved predictions are available in the open literature. Most of the previous predictive studies have attempted to replicate time-mean experimental data. For example, Ameri and Bunker [2] performed computations for the flow in a linear cascade typical of a first-stage power generation turbine. This was a simulation of the experiment of Bunker et al. [3] that obtained nearly full surface heat transfer data on flat tips with various edges, three clearances, and two turbulence levels. The simulation compared favorably with the data. Also, Moore et al. [4] studied flat tip region flows from incompressible laminar to turbulent transonic conditions and compared their predictions of flow characteristics and heat transfer with available experimental data. Some have also attempted to predict the flow and heat transfer in full scale, rotating turbine rigs. Metzger et al. [5] performed predictions of the data taken by Dunn et al. [6a, 6b] on the Garrett 731-2 turbine. They showed that a simple model describing the tip flow could be used to predict the time-averaged tip and BOAS heat transfer once the leakage flow-rate was estimated. Ameri and Steinthorsson [7] also made predictions of the time-averaged heat transfer of the Dunn et al. [6a, 6b] experiment and showed good agreement with the experimental results. Several recent experimental studies have reported heat transfer and cooling effectiveness in the vicinity of blade tips in cascades [8-10], but perhaps the most relevant investigation to the current study was performed by Chana and Jones [11]. The authors' measurements provided new insights into the blade outer air-seal flow, and they revealed high unsteadiness in the tip region both in pressure and in heat transfer. They also suggested that an unsteady oscillation in heat transfer to and from the blade BOAS exists with each blade passage.

In the present study, a detailed comparison of time-resolved measurements and Reynolds Averaged Navier-Stokes (RANS) predictions of pressure and heat transfer on a blade outer air seal is

presented. The measurements were conducted in the Turbine Research Facility (TRF) at Wright-Patterson Air Force Base. All details of the short-duration experimental technique and the transonic turbine are presented in Polanka et al. [12], and further comparisons of data and prediction (e.g. on the blade tip) are given in a companion paper [13]. The turbine represents a modern single-stage high pressure turbine used for military aircraft application. The blade-tip geometry is flat with a nominal clearance of 0.24 mm (approximately 0.5% of trailing-edge span). For the pressure measurements reported here the method of Kline and McClintock [14] resulted in ± 0.45% uncertainty while the turbine total quantities had ± 0.15% uncertainty. Further, a jitter analysis as described by Moffat [15] was performed through the heat-flux data-reduction algorithm to obtain the uncertainty in the surface heat transfer. This varied from gauge to gauge, but did not exceed 4% of the mean levels presented here. What follows is a detailed comparison between the experimental data and a prediction at the turbine design condition.

NOMENCLATURE

k	Thermal conductivity (kW/m-K)
n	Normal distance from a solid boundary (m)
P	Pressure (kPa)
$q"$	Heat flux (kW/ m^2)
T	Temperature (K)
x / b_x	Fraction of blade axial chord
y^+	Law-of-the-wall variable

Subscripts

aw	Adiabatic wall
in	Inlet
s	Static properties
t	Total properties
w	Wall

COMPUTATIONAL METHODS

Steady-state pressure fields and wall heat fluxes in the single stage, transonic turbine were predicted using the 3-D, Reynolds-Averaged Navier-Stokes (RANS) code described collectively by Ni [16, 17], Ni and Bogoian [18], and Davis et al. [19]. The code employed a finite volume, cell centered, Lax-Wendroff [20] method and was accurate to second order in both space and time. Numerical closure was obtained

with the high Reynolds number k-ω turbulence model as described by Wilcox [21], and multi-grid techniques were used to obtain rapid convergence. Consistent with the experiment, an isothermal boundary condition was imposed on all solid boundaries, and these were also treated as no-slip surfaces. Turbulent flow was assumed throughout, and the inlet boundary layer was allowed to grow over a distance consistent with the inlet flowpath of the rig.

Single-stage, steady-state calculations were performed with 44 vanes and 58 blades as per the experiment. For such steady-state calculations, the Ni code employs a mixing-plane approximation to transfer information across the inter-row boundary (See Ni [16]). In this instance the mixing plane approximation consists of circumferentially averaging the 2D exit flowfield from the vane row and mapping 1D profiles onto the inlet boundary of the downstream blade row. For these calculations an OH grid topology was employed, and the grid counts used to model each airfoil passage and the tip clearance region are listed in Table 1. These grid counts were consistent with standard work criteria defined by Praisner [22] at Pratt & Whitney to capture properly the thermal fields in modern gas turbines. The P&W design viscous grid was defined to produce near surface values of y^+ less than 1 over all no-slip boundaries as recommended by Dunham and Meauze [23] for use with two-equation turbulence models. Also, the grid gave approximately 15 grid points in the boundary layer on each airfoil surface.

Table 1. Grid counts used for the 3D RANS simulations.

Axial x Radial x Circumferential Grid Counts:

O-Mesh	113x33x57	113x33x57[*]
H-Mesh	185x33x57	169x33x57

[*] Each blade also had a 57x32x32 Tip-Clearance Grid

The 3D steady flowfields predicted by the flow solver were post-processed to allow for direct comparisons with time-resolved experimental pressure and heat transfer distributions on the blade outer air-seal. The majority of the post-processing was straightforward, but some of it requires clarification. For example, the conclusion of Prasad and Wagner [24] that the time-resolved pressure on the turbine BOAS

was consistent with the periodic passing of a flowfield that was steady in the blade frame of reference was assumed to be valid. Consequently, it was possible to compare both time-resolved experimental pressures and heat fluxes on the BOAS with the steady-state predictions, as will be shown. Careful attention was paid to the frequency content of the experimental data, and the predicted signals were low-pass filtered to ensure a consistent comparison where appropriate. Finite impulse response (FIR) digital filters were employed to ensure that the phase angles of all fluctuations were preserved over the pass band of the filter. Also, the values of the predicted wall heat flux that were compared to experimental data were calculated via a heat balance applied across the first computational cell in the direction normal to and into the wall, namely

$$q'' = -k\,(\,T_w - T_s\,)\,/\,\Delta\,n \quad . \tag{1}$$

In the above relation, the thermal conductivity of air, k, was evaluated at the film temperature $(T_s + T_w)\,/\,2$ and $\Delta\,n$ was the distance between the first two grid points adjacent to the wall and normal to it. The driving temperature, T_s, was the local static temperature, and T_w was the wall temperature.

It should be noted that the computational results presented below are from true predictions of the flowfield. That is, a design grid was generated for the single-stage turbine geometry, a set of boundary conditions from a single experiment conducted in the TRF were mapped onto the computational domain, and the flow solver was exercised. The relevant boundary conditions included the measured upstream total pressure (383 kPa) and total temperature (449 K), the downstream static pressure (107 kPa), the wheel speed (7500 rpm), and the time-mean wall temperature over the experimental test window (362 K). The boundary conditions were taken as measured time-average values for 100ms of the total run time of the experiment. Over that interval the upstream total quantities, the wheel speed, and the wall temperature on the BOAS varied by less than 1% while the downstream static pressure varied 1.3%. The free-stream turbulence intensity was taken to be 2%, and that was in keeping with previous measurements in the TRF. The turbulence intensity sets the boundary condition on k, and the boundary condition for ω was set to ensure a turbulent length scale of order 10% of the span at the leading edge of the vane [22]. This investigation focused only on the baseline run described in Polanka et al. [12], where the relevant similarity

parameters for the engine are a gas-to-metal temperature ratio of 1.47, a total-to-total pressure ratio of 2.76, a corrected speed of 0.57 (mid-span tangential velocity divided by sonic speed at inlet), and an exit Reynolds number based on axial chord of 3.80×10^5.

RESULTS

Figure 1 is a pair of plots giving the predicted distributions of static pressure and wall heat-flux on the BOAS. The local static pressure is normalized by the turbine-inlet total pressure to give an indication of the local absolute Mach number through the turbine blade row while the local wall heat-flux is plotted in kW/m^2. The heat flux is plotted in its raw form purposefully: a true physics-based durability design system implies a capability to predict accurately the local cooling requirements of hot section parts. Toward this end, validation is taken here to mean a comparison of predicted and measured raw heat fluxes without invocation of any heat-transfer coefficient. Discrete static-pressure measurements were taken with high response, surface mounted Kulite transducers at the axial stations indicated on Fig. 1, while heat fluxes were measured at equivalent axial locations using button-type thin-film gauges as described by Dunn [1] (See also Schultz and Jones [25]). The characteristics of the specific gauges used here were reported by Weaver et al. [26]. The substrate buttons were approximately 3mm thick, so the semi-infinite assumption employed to reduce the heat-flux data was well justified over the experimental time interval studied here ($\approx$1s after flow start). Also, ohmic heating of the gauges by the sensing current applied to them resulted in a very small change in surface temperature (< 0.1 K). Again, the flow over the BOAS was considered to be steady in the blade frame of reference. In the stationary frame of reference a fixed sensor was therefore in an unsteady flowfield. Accordingly, the steady RANS predictions in Fig. 1 were translated to the stationary frame of reference for comparison with true time-resolved measurements on the BOAS.

Time-Resolved Pressure

Figure 2 is a plot of the time-resolved pressure for the four BOAS gauges as compared to the time-resolved experimental data. Also shown on the figure are the times that the blade pressure and suction surfaces were at each gauge location. The prediction and the data compare quite well in terms of the peak-to-peak variation over a blade-passing period and in terms of the DC level (i.e. the time mean). Both the

predicted and experimental traces also have a steep rise in level after the passage of the tip pressure side followed by a decrease as the blade passage traversed the sensor. However, the predicted time trace is characterized by an increase in pressure across the tip followed by a decrease as the pressure side of the tip passed over the gauge. The experimental data suggests a more constant pressure as the tip passed over the gauge. In contrast, the experimental data of Chana and Jones [11] and Prasad and Wagner [24] revealed more of the variation evident in the current prediction.

Time-Resolved Heat Transfer

While the time-mean BOAS pressure distribution was accurately predicted with the 3-D RANS solver, the time-mean heat transfer was substantially over-predicted, as seen in Fig. 3. In the figure, a set of time-resolved heat fluxes on the BOAS for the five thin-film gauges used in the experiment is shown. For each gauge, both the experimental data and the predictions are plotted. The experimental data was not ensemble averaged in any way before plotting: instead, it is shown as raw data. So, some a-periodicity is evident in the experiment but not in the computation. The ordinate for each plot is heat flux, while the abscissa is time non-dimensionalized by the period of blade passing. Again, raw heat-flux levels were plotted purposefully without the benefit of ensemble averaging. This is because the end goal of this study was a validation of calculated heat-flux levels for a given set of boundary conditions. This is a necessary capability if a durability designer is to determine film-cooling requirements for a BOAS during the design cycle. Also plotted on the figure are vertical lines representing the predicted times that the blade tip pressure- and suction-side are over the heat-flux gauge. Note that, for all gauges, the predicted heat flux is a maximum when the blade tip pressure-side is over the heat-flux gauge, when a very large excursion from the mean level occurs. This makes physical sense because the boundary layer on the BOAS is greatly energized by the tip-clearance flow as it comes over the tip from the pressure side. So, the attendant thinning of the boundary layer on the BOAS resulting from this effect should be associated with very high levels of both shear stress and heat flux.

The prediction reveals higher frequency content with each blade passing than was observed in the experiment. To investigate this, Discrete Fourier Transform (DFT) magnitudes for both the measurement and computation at $x / b_x = 0.56$ are shown in Fig. 4. Note that the abscissa of the plot is engine order

which is a frequency normalized by the number of rotor revolutions per second. Since there are 58 turbine blades around the rotor circumference, the first blade passing frequency occurs at engine order 58. The predicted heat-flux variation on the BOAS is derived from the full spatial (and hence both temporal and spectral) resolution of the simulation (355 kHz), and very high harmonics of the blade passing frequency are evident in the plot. Such high harmonics are not typically seen in time-resolved predictions of vane-blade interaction [27], and this is an indication that the validation of the BOAS prediction may require an increase in the bandwidth of heat flux measurements relative to the state of the art.

From inspection of Fig. 3, it is clear that both the peak level of the predicted signals and the time-mean levels are lower in the experiment relative to the prediction. From the point of view of the turbine durability engineer, accurate prediction of the time-mean heat flux is paramount. The mean level of the computation is clearly affected by the frequency content of the signal, and this suggests that very high frequencies must be resolved in experiments to validate the prediction properly. Therefore, it becomes important to determine whether or not the high frequency components of the predicted signal over the blade tip are truly characteristic of this flowfield. In the TRF, time-resolved temperature signals are recorded and subsequently processed into time-resolved heat fluxes by solving the 1-D unsteady heat conduction equation. As clearly shown by Oldfield [28], a thin-film gauge response is frequency dependent, and high frequency fluctuations in heat flux can be lost unless a significant fraction of the A/D input range is used to capture the AC portion of the temperature signal. All the temperature signals obtained for this study were conditioned through DC-coupled amplifiers that had a flat frequency response in the Bessel filter pass-band prior to digitization. So, it is possible that a systematic error in the experiment accounts for both the lack of high frequency components in the data and the over-prediction of the time-mean heat flux on the BOAS.

It is possible to determine the effects of the measurement technique on the frequency content of the BOAS heat-flux with some rigor. If one considers the predicted time variation of heat flux to be accurate, it is possible to calculate the predicted time history of the substrate surface temperature that would result from that heat flux by invoking the 1D unsteady heat-conduction equation and solving it numerically. One can then assess the effects of A/D resolution and low-pass filtering on the measured temperature and reconstruct the predicted heat-flux traces that would result from those operations to compare with the true measured variation. This was done, and the results are plotted in Fig. 5 for the thin-film gauge at x /

b_x=0.56. In the topmost panel of the figure, two predicted surface-temperature histories are shown. One temperature history takes the A/D resolution into account (0.0164 K / count at 12 bits of resolution) and the other includes the effect of low-pass filtering at 20 kHz before acquisition. Heat-flux traces are also plotted in the central panel of Fig. 5. The time-history predicted directly by the 3D RANS solver is shown along with the experimental data. Also plotted are heat-flux traces determined by re-processing the predicted surface-temperature histories via the method of Cook and Felderman [29]. Note that the A/D resolution in temperature is adequate to reproduce the frequency content of the RANS-predicted heat flux, but low-pass filtering the temperature trace before acquisition brings the predicted heat flux into much closer agreement with the actual measurements.

So, it is clear that the discrepancies between the experiment and prediction as regards frequency content as well as maximum and mean levels can be a consequence of the measurement system. This is not to say that the RANS solver and the turbulence model used in conjunction with it are perfectly adequate to predict the BOAS heat-transfer variation. However, the results of this exercise do help to explain why the disagreement between measurement and prediction is so large. Further, giving the predictive tool the benefit of the doubt when comparing predictions to experimental results has yielded a means whereby future measurements can be improved. This should aid in closing the gap between experiment and prediction for this complicated flowfield.

Note that for some portion of the blade-passing period the measured heat flux on the BOAS is negative, and this is quite inconsistent with what occurs in the engine situation. Negative levels of heat flux are sometimes seen in data derived from wall temperature measurements via the technique of Cook and Felderman [29] as a consequence of the differentiation operation concomitant with the method, but they do not typically persist from blade passing to blade passing as seen here [30]. So, the negative heat fluxes here are an indication that the local recovery temperature is less than the wall temperature over that same interval. Although the turbine-inlet temperature (449K) is elevated relative to the pre-test wall temperature (362K), the upstream total temperature was limited by the tight running clearance (0.24mm) of the turbine and the need to achieve the design corrected speed of the motor. Since the flow through the rig is diabatic and enthalpy is extracted from the flow by the turbine blade, the local recovery temperature over the BOAS becomes smaller than the local wall temperature for some portion of each blade passing period.

For the same reason, the local static temperature over the BOAS in the laminar sub-layer is smaller than the local surface temperature. The heat flux then becomes negative as defined by Equation 1, and this is representative of heat transfer *from* the BOAS to the freestream during a portion of the blade-passing interval.

Note that this phenomenon occurs in the prediction as well as in the experiment. To show this, a separate adiabatic wall simulation was run in order to determine the driving temperature at the solid boundary. The predicted time history of the heat transfer driving potential over the thin-film gauge located at $x/b_x = 0.56$ is shown in the bottom panel of Fig. 5. Here the difference between the local adiabatic wall temperature in the absolute frame of reference and the wall temperature from the isothermal simulation was taken as the driving potential. As shown, negative heat flux results for both the prediction and the experiment at time windows consistent with the negative predicted driving potential. Again for the BOAS this was physically realistic given the relatively low turbine-inlet temperature combined with both the diabatic nature of the flowfield and the extraction of energy from the flow by the turbine blade.

CONCLUSIONS

This work compared experimental data taken on the BOAS of a full-scale, rotating turbine stage with a prediction of the flowfield made with a 3-D RANS solver. While differences in magnitude occurred between the prediction and the experimental data, particularly with respect to heat transfer, the general trends were consistent. Also, the predicted time-history of heat flux on the BOAS was characterized by very high levels of heat transfer as the pressure side of the blade tip passed over the gauges. Consequently, very high frequencies and high amplitude fluctuations were observed in the predicted signals that were not observed in the experiment. These large amplitude fluctuations were physically realistic, and processing the predicted time-resolved heat-flux in a manner consistent with the experiment revealed that both the peak and the time-mean levels on the BOAS could be as high as was predicted. So, instrumentation developments are underway to improve the bandwidth of heat-flux measurements for future tests. Finally, using the results of the predictions, the driving temperature for BOAS heat transfer was investigated. It was shown that the local adiabatic wall temperature of the flow in the vicinity of the BOAS fluctuated with time and can result in a negative heat transfer driving potential (and hence heat flux).

REFERENCES

[1] Dunn, M.G., 2001, "Convective Heat Transfer and Aerodynamics in Axial Flow Turbines," ASME Paper No. 2001-GT-0506.

[2] Ameri, A.A., and Bunker, R.S., 2000, "Heat Transfer and Flow on the First-Stage Blade Tip of a Power Generation Gas Turbine: Part 2 -Simulation Results," ASME Journal of Turbomachinery, Vol. 122, pp. 272-277.

[3] Bunker, R.S., Bailey, J.C., and Ameri, A.A., 2000, "Heat Transfer and Flow on the First-Stage Blade Tip of a Power Generation Gas Turbine: Part 1 -Experimental Results," ASME Journal of Turbomachinery, Vol. 122, pp. 263-271.

[4] Moore, J., Moore, J.G., Henry, G.S., Chaudhry, U., 1989, "Flow and Heat Transfer in Turbine Tip Gaps," ASME Journal of Turbomachinery, Vol. 111, pp. 301-309.

[5] Metzger, D.E., Dunn, M.G., and Hah, C., 1991, "Turbine Tip and BOAS Heat Transfer," ASME Journal of Turbomachinery, Vol. 113, pp. 502-507.

[6a] Dunn, M.G., Rae, W.J., and Holt, J.L, 1984, "Measurement and Analyses of Heat Flux Data in a Turbine Stage: Part I-Description of Experimental Apparatus and Data Analysis," ASME Journal of Engineering for Gas Turbines and Power, Vol. 106, pp. 229-233.

[6b] Dunn, M.G., Rae, W.J., and Holt, J.L, 1984, "Measurement and Analyses of Heat Flux Data in a Turbine Stage: Part II-Discussion of Results and Comparison With Predictions," ASME Journal of Engineering for Gas Turbines and Power, Vol. 106, pp. 234-240.

[7] Ameri, A.A. and Steinthorsson, E., 1996, "Analysis of Gas Turbine Rotor Blade Tip and BOAS Heat Transfer," ASME Paper No. 96-GT-189.

[8] Christophel, J. R., Couch, E., Thole, K. A., and Cunha, F. J., 2004, "Measured Adiabatic Effectiveness and Heat Transfer for Blowing from the Tip of a Turbine Blade," ASME Paper No. GT2004-53250.

[9] Nasar, H., Ekkad, S. V., and Bunker, R. S., "Effect of Tip and Pressure Side Coolant Injection on Heat Transfer Distributions for a Plane and Recessed Tip," ASME Paper No. GT2005-68595.

[10] Mhetras, S., Yang, H., Gao, Z., and Han, J. C., "Film Cooling Effectiveness on Squealer Rim Walls and Squealer Cavity Floor of a Gas Turbine Blade Tip Using Pressure Sensitive Paint," ASME Paper No. GT2005-68387.

[11] Chana, K.S. and Jones, T.V., 2002, "An investigation On Turbine Tip and BOAS Heat Transfer," ASME Paper No. GT2002-30554.

[12] Polanka, M.D., Hoying, D.A., Meininger, M., and MacArthur, C.D., 2003, "Turbine Tip and BOAS Heat Transfer and Loading Part A: Parameter Effects Including Reynolds Number, Pressure Ratio and Gas to Metal Temperature Ratio", ASME Journal of Turbomachinery, Vol. 125, pp. 97-106.

[13] Polanka, M. D., Clark, J.P., White, A. L., Meininger, M., and Praisner, T. J., 2003, "Turbine Tip and BOAS Heat Transfer and Loading, Part B: Comparisons Between Prediction and Experiment, Including Unsteady Effects," ASME Paper No. GT2003-38916.

[14] Kline, S. J. and McClintock, F. A., 1953, "Describing Uncertainties in Single Sample Experiments," Mechanical Engineering, Vol. 75, pp. 3-8.

[15] Moffat, R. J., 1982, "Contributions to the Theory of Single-Sample Uncertainty Analysis," Journal of Fluids Engineering, Vol. 107, pp. 153-160.

[16] Ni, R.H., "Advanced Modeling Techniques for New Commercial Engines," 1999, XIV ISOABE Conference, Florence, Italy, 5-10 September.

[17] Ni, R. H., 1982, "A Multiple-Grid Scheme for Solving the Euler Equations," AIAA Journal, Vol. 20, No. 11, pp. 1565-1571.

[18] Ni, R. H. and Bogoian, J. C., "Prediction of 3-D Multistage Turbine Flow Field Using a Multiple-Grid Euler Solver," AIAA Paper No. 89-0203.

[19] Davis, R. L., Shang, T., Buteau, J., and Ni, R. H., 1996, "Prediction of 3-D Unsteady Flow in Multi-Stage Turbomachinery Using an Implicit Dual Time-Step Approach," AIAA Paper No. 96-2565.

[20] Lax, P. D., and Wendroff, B., 1964, "Difference Schemes for Hyperbolic Equations with High Order Accuracy," Communications on Pure and Applied Mechanics, Vol. 17, pp. 381-398.

[21] Wilcox, D.C., 1998, Turbulence Modeling for CFD, Second Edition, DCW Industries, Inc., La Canada, California.

[22] Praisner, T.J., 2001, Personal Communication.

[23] Dunham, J. and Meauze, G., 1998, "An AGARD Working Group Study of 3D Navier-Stokes Codes Applied to Single Turbomachinery Blade Rows," ASME Paper No. 98-GT-50.

[24] Prasad, A. and Wagner, J.H., 2000, "Unsteady Effects in Turbine Tip Clearance Flows," ASME Journal of Turbomachinery, Vol. 122, No. 4, pp. 621-627.

[25] Schultz, D. L. and Jones, T. V., 1973, "Heat Transfer Measurements in Short-Duration Hypersonic Facilities," NATO AGARDOGRAPH 165.

[26] Weaver, M. W., Moselle, J. R., Dunn, M. G., and Guenette, G. R., 1994, "Reduction of Data From Heat-Glux Gauges -- A Documentation of the MIT ACQ Code and an Adaption to Single-Sided Gauges," Calspan Report No. 7733-4.

[27] Clark, J. P. and Grover, E. A., 2006, "Assessing Convergence in Predictions of Periodic-Unsteady Flowfields," ASME Paper No. GT2006-90735.

[28] Oldfield, M.L.G., 1988, "Experimental Techniques in Unsteady Flows," Oxford University Engineering-Laboratory Report 1843/90.

[29] Cook, W. J. and Felderman, E. J., 1966, "Reduction of Data from Thin-Film Heat-Transfer Gauges: A Concise Numerical Technique," AIAA Journal, Vol. 4, No. 3, pp. 561-562.

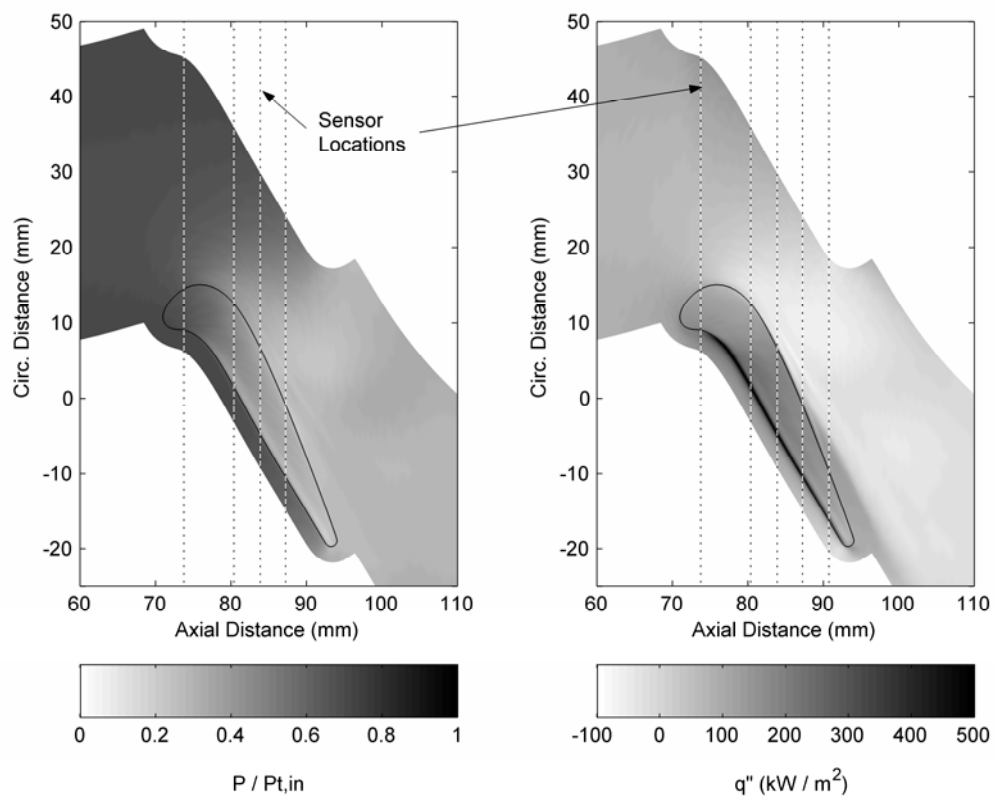[30] Dunn, M. G., 2005, Personal Communication.

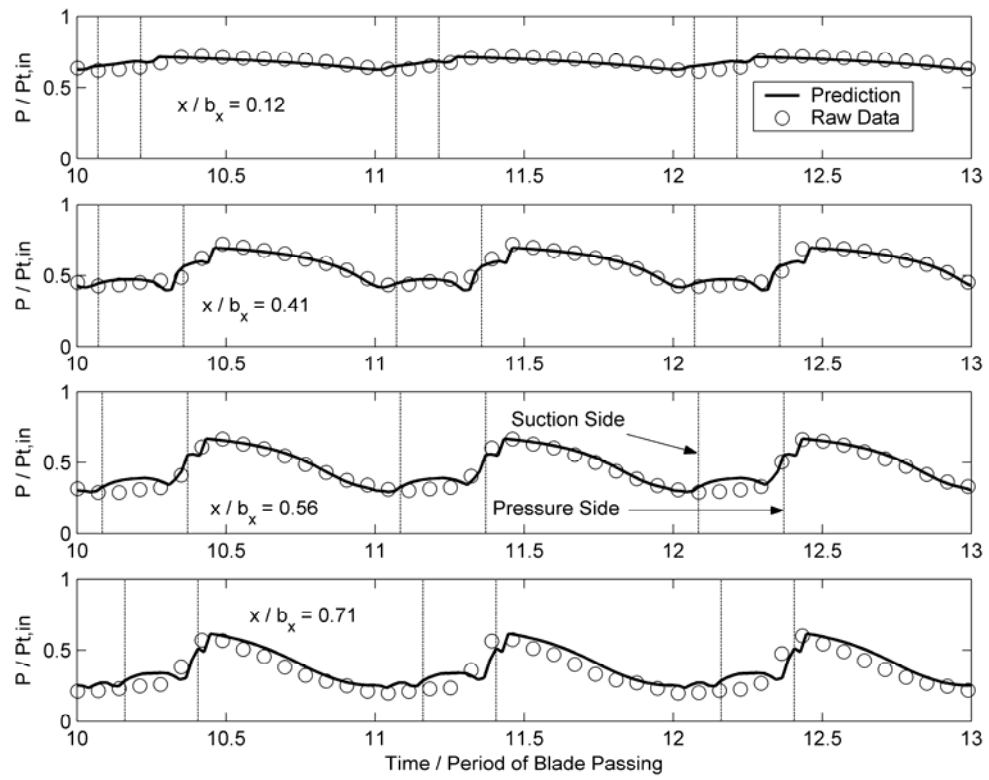Figure 1. Predicted BOAS static pressure and heat-flux distributions.

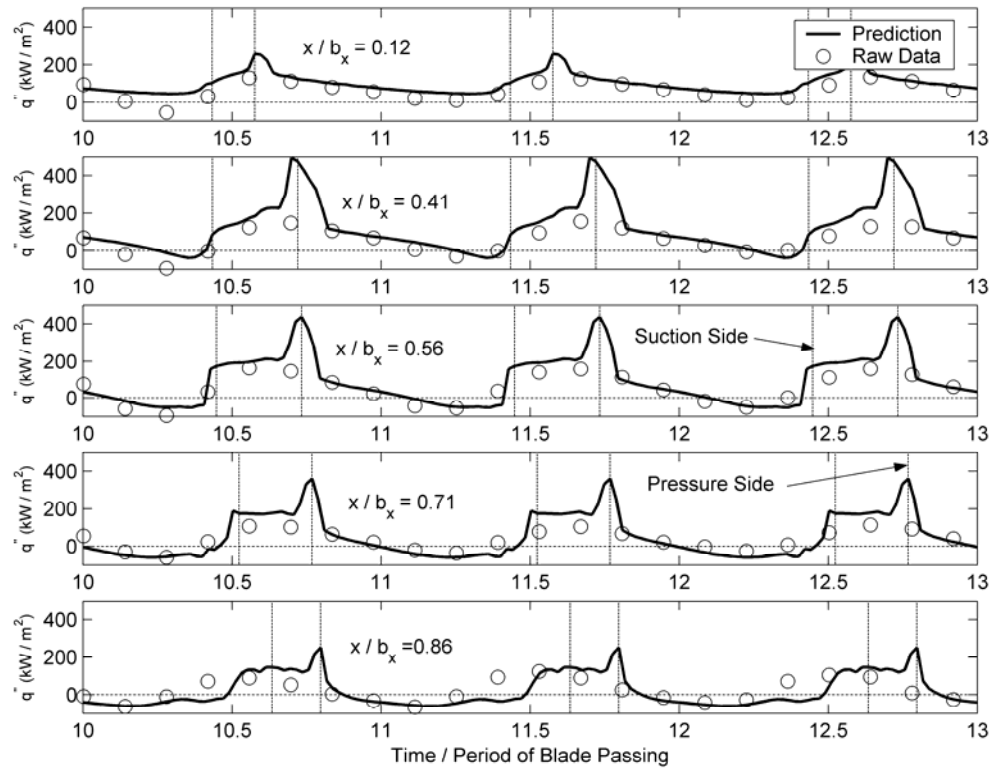Figure 2. A comparison of measured and predicted time-resolved static pressures on the BOAS.

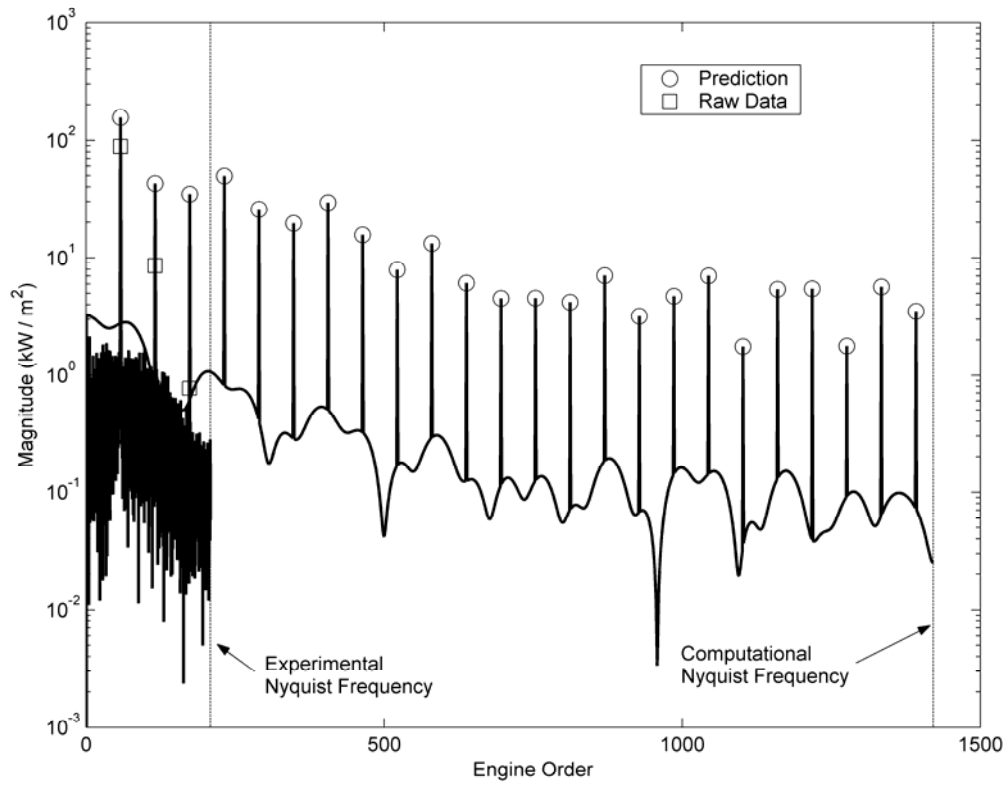Figure 3. A comparison of measured and predicted time-resolved heat fluxes on the BOAS.

Figure 4. A comparison of Discrete Fourier Transform (DFT) magnitudes from the measured and predicted heat flux variations on the BOAS at $x / b_x = 0.56$.
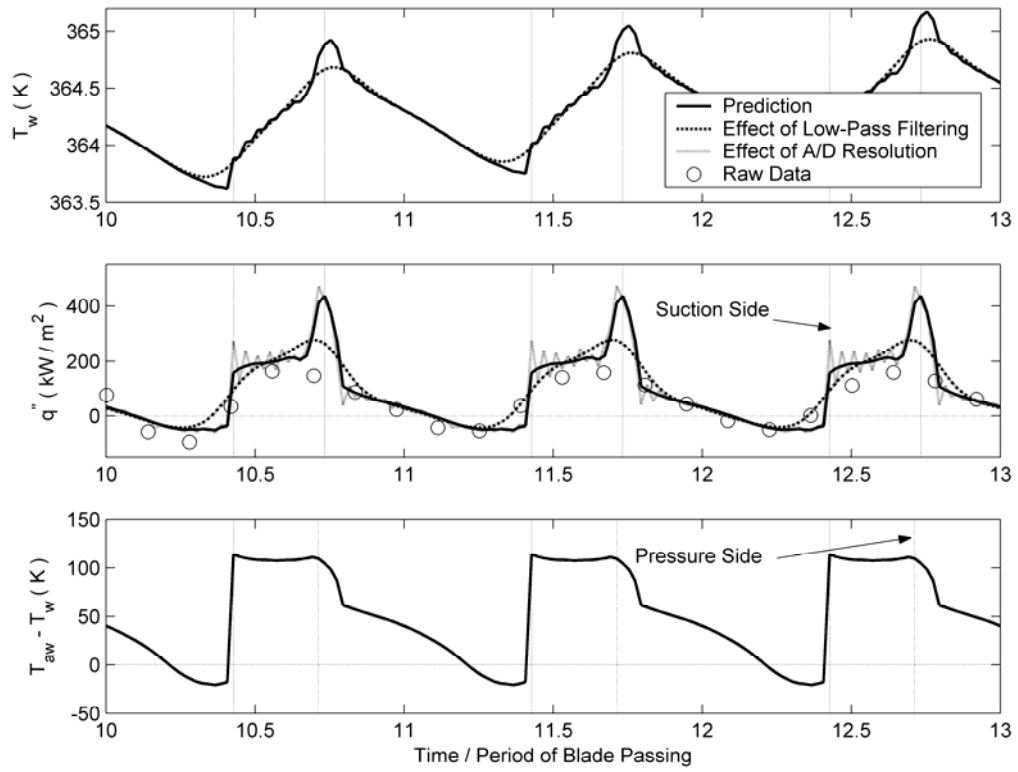
Figure 5. An assessment of A/D resolution and low-pass filtering on the predicted BOAS surface temperature with attendant effects on the apparent measured wall heat-flux. Also, the time history of the heat-flux driving potential is shown. All signals are for the gauge at $x / b_x = 0.56$.